

Flow of a visco-plastic fluid in a channel of slowly varying width

I.A. Frigaard^{a*}, D.P. Ryan^b

^a Departments of Mathematics and Mechanical Engineering, University of British Columbia, 2324 Main Mall, Vancouver, BC, Canada V6T 1Z4

^b Department of Mathematics, University of British Columbia, 1984 Mathematics Road, Vancouver, BC, Canada V6T 1Z2

Received 13 February 2004; received in revised form 23 June 2004

Abstract

We develop an asymptotic solution for the Poiseuille flow of a Bingham fluid along a two-dimensional channel of slowly varying width, for the case of small amplitude width variation, h . We show that an asymptotic solution with an intact unyielded plug region can be found for h less than a critical value $h_c \sim O(\delta)$, where δ is the aspect ratio (channel half-width to wavelength of the variation). Our method involves no form of relaxation of the exact Bingham model.

We provide upper and lower estimates for h_c . The function h_c/δ shows little variation with $\delta \ll 1$, and exhibits a maximum in Bingham number, B , at around $B \approx 5$. There is a small variation in the true plug speed from that of the uniform channel flow. At small B the perturbed plug moves slightly slower than that in the uniform channel, whereas at large B the true plug moves faster than the uniform channel flow. Finally, we consider the structure of the flow for $h \sim O(1)$, for which the plug has broken.

© 2004 Elsevier B.V. All rights reserved.

Keywords: Lubrication theory; Visco-plastic fluids; Extensional flows; Pseudo-yield surfaces; Pseudo-plugs

1. Introduction

In this paper, we develop an asymptotic solution for the Poiseuille flow of a Bingham fluid along a two-dimensional channel of slowly varying width, for the case of small amplitude width variation, h , see Fig. 1. The flow of a Newtonian fluid along a wavy-walled rigid channel, in its various limits, has been studied by many authors, and has effectively become a textbook problem. For a Bingham fluid these same problems can of course be attempted, but here we have a specific objective in mind: namely, to understand what happens to the unyielded plug region under a small perturbation of the channel width.

Analyses of visco-plastic fluid flows in geometries of small aspect ratio have a relatively long history. Part of the interest is in what has become known as the *lubrication paradox* for yield stress fluids, which refers to the existence or non-existence of a true unyielded plug region. It was perhaps Lipscomb and Denn [1], who first aroused interest in this question by arguing that true rigid plug regions should not ex-

ist in complex geometries, with reference to a squeeze flow. The argument is that adoption of classical lubrication, (or thin-film), scaling techniques leads to prediction of a *plug-speed* which varies slowly in the principal flow direction. This variation implies that the plug region cannot be truly unyielded. Such regions have been termed *pseudo-plug* regions and the boundaries either *pseudo-yield* surfaces or *fake yield* surfaces.

There have been a number of attempts to resolve the paradox. Certainly, both analytical and computational methods have shown that true unyielded plugs can exist in complex geometries. The chief value of [1] was however to draw attention to the potential difficulties of these flows, rather than offering a resolution. Probably the earliest demonstration of a true unyielded plug in a slowly varying complex geometry was by Walton and Bittleston [2], who studied the axial flow of a Bingham fluid along an eccentric annular duct. It was shown analytically [2] (and later confirmed computationally [3]), that a true plug can persist in the middle of the channel, on both the wide and narrow side of the eccentric annulus. Between the two rigid plug zones there exists a pseudo-plug region, where the scaled velocity gradient is asymptotically small in the shear direction (across the annu-

* Corresponding author. Tel.: +1 604 822 6074.

E-mail address: frigaard@mech.ubc.ca (I.A. Frigaard).

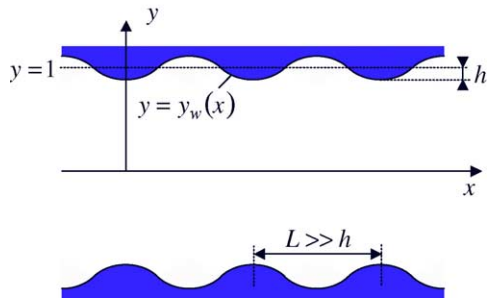


Fig. 1. Slowly varying channel geometry.

lus), but exhibits an order unity variation in the extensional direction (the azimuthal direction). What is noteworthy about these two papers is that neither the analytical method in [2] nor the numerical method in [3] rely on any form of regularisation (or smoothing) of the effective viscosity of the exact Bingham model.

In the context of the lubrication paradox, squeeze flow problems have attracted considerable attention over the years, e.g. [1,4–10]. In an axisymmetric geometry, it may be shown by symmetry arguments that true plug regions exist in an $O(1)$ region close to the axis of symmetry, at the stagnation points, see [10]. True plugs do not however exist in the radially developing shear flow. In the shear flow region, the mean velocity decreases slowly with radial distance. Thus, there is an imposed extensional strain and this prevents formation of a true plug.

A similar situation is found in thin film flows of viscoplastic fluids down inclined planes, of which there are many practical examples, e.g. [11–26], stemming from both geophysical and industrial scenarios. In these flows there is generally a slow variation in film thickness in the direction of flow. Since the film height determines the leading order velocity solution, there is again a slow extensional stretching of the (pseudo-)plug velocity in the flow direction and no true plug. An exception to this is when the layers become so thin that they do not move. In this situation, the pseudo-plug velocity is zero everywhere and hence the troublesome extensional gradient is removed.

There have been two attempts at an asymptotic analysis of these flows, to resolve the lubrication paradox: by Wilson [20], and by Balmforth and Craster [19]. The former method relies on relaxation of the exact Bingham model to a bi-viscosity model, followed by consideration of a distinguished limit of the bi-viscous model. We review Wilson's method later in the context of our results, in appendix Appendix A. The latter method [19], is more in the spirit of our analysis, and the earlier analysis in [2]. No relaxation/regularisation is used (or needed). The results are thus fully consistent with the exact Bingham model.

Here, we consider perturbation of a plane channel Poiseuille flow of a Bingham fluid, via slow length-wise variation of the channel width. In a uniform channel, the Poiseuille flow has a finite width unyielded plug region. For

an infinitesimal perturbation of the channel wall, one would expect that the unyielded plug will remain. This might appear to be in contradiction to the above analyses of slowly varying shear flows, both in squeeze films and in thin film flows down an incline. However as we have explained, in the above two cases there is a persistent variation of the velocity in the flow direction, i.e. an extensional rate of strain, that does not change sign in the flow direction. For a channel flow, with periodic variation of the channel width, the extensional strain rate should change sign along the channel. This allows the plug to persist for sufficiently small amplitude wall variations, as we shall demonstrate.

An outline of the paper is as follows. The lubrication model is described below in Section 2. Section 3 is the main section of the paper and develops the asymptotic approximation for small amplitude width variations. Eventual breaking of the plug and prediction of the critical amplitude is in Section 4, where we also discuss the flow structure after the plug has broken. The paper concludes with a brief discussion. In a short appendix Appendix A we review Wilson's method of distinguished limits for the bi-viscous model, as applied to our situation, showing that the predictions are contradictory.

2. Flow of a visco-plastic fluid in a channel of slowly varying width

Consider the flow of an incompressible Bingham fluid along a two-dimensional channel of slowly varying width. We adopt a classical lubrication scaling (defined below), to arrive at the following system of dimensionless equations:

$$\delta Re \left(\frac{\partial u}{\partial t} + u \frac{\partial u}{\partial x} + v \frac{\partial u}{\partial y} \right) = -\frac{\partial p}{\partial x} + \delta^2 \frac{\partial}{\partial x} \tau_{xx} + \frac{\partial}{\partial y} \tau_{xy}, \quad (1)$$

$$\delta^3 Re \left(\frac{\partial v}{\partial t} + u \frac{\partial v}{\partial x} + v \frac{\partial v}{\partial y} \right) = -\frac{\partial p}{\partial y} + \delta^2 \frac{\partial}{\partial x} \tau_{xy} + \delta^2 \frac{\partial}{\partial y} \tau_{yy}, \quad (2)$$

$$\frac{\partial u}{\partial x} + \frac{\partial v}{\partial y} = 0. \quad (3)$$

The x -coordinate is aligned with the channel axis, $\mathbf{u} = (u, v)$ is the velocity, p is the pressure and τ_{ij} is the deviatoric stress tensor. We have scaled lengths in the x & y -directions differently, with the wavelength \hat{L} , of the channel width variation, and with the channel half-width \hat{D} , respectively. The aspect ratio δ , and Reynolds number Re , are defined by:

$$\delta \equiv \frac{\hat{D}}{\hat{L}}, \quad Re \equiv \frac{\hat{\rho} \hat{U}_0 \hat{D}}{\hat{\mu}}, \quad (4)$$

where $\hat{\rho}$, \hat{U}_0 , and $\hat{\mu}$ are respectively the density, mean flow velocity in the x -direction and plastic viscosity, (all dimensional). To derive the non-dimensional field equations above, the velocity components in the x and y -directions are scaled

with \hat{U}_0 and $\delta\hat{U}_0$, respectively. The pressure is scaled with $\hat{\mu}\hat{U}_0/\hat{D}$. The shear-stress components $\tau_{xy}(= \tau_{yx})$, have also been scaled with $\hat{\mu}\hat{U}_0/\hat{D}$. The extensional stresses $\tau_{xx}(= -\tau_{yy})$, are scaled with $\delta\hat{\mu}\hat{U}_0/\hat{D}$.

We consider the formal limit $\delta \ll 1$. Eqs. (1)–(3) are the standard lubrication equations for any generalised Newtonian fluid. Here, we consider a Bingham fluid, for which the constitutive laws are:

$$\tau_{ij} = \left(1 + \frac{B}{\dot{\gamma}}\right) \dot{\gamma}_{ij} \iff \tau > B \quad (5)$$

$$\dot{\gamma} = 0 \iff \tau \leq B, \quad (6)$$

where

$$\begin{aligned} \dot{\gamma}_{xy} = \dot{\gamma}_{yx} &= \frac{\partial u}{\partial y} + \delta^2 \frac{\partial v}{\partial x}, & \dot{\gamma}_{xx} &= 2 \frac{\partial u}{\partial x} = -2 \frac{\partial v}{\partial y} = -\dot{\gamma}_{yy}, \\ \dot{\gamma} &= [\dot{\gamma}_{xy}^2 + \delta^2 \dot{\gamma}_{xx}^2]^{1/2}, & \tau &= [\tau_{xy}^2 + \delta^2 \tau_{xx}^2]^{1/2}. \end{aligned} \quad (7)$$

The dimensionless number appearing above is the Bingham number, B :

$$B \equiv \frac{\hat{\tau}_Y \hat{D}}{\hat{\mu} \hat{U}_0}, \quad (8)$$

where $\hat{\tau}_Y$ is the yield stress. The Reynolds number is well known and δ requires no explanation. The Bingham number physically represents the ratio of yield stress to viscous stress. In a plane channel flow the Poiseuille flow solution contains an unyielded plug zone at the centre of the channel, of width $2y_{y,0}$, where $y_{y,0}$ is determined solely by B . As $B \rightarrow \infty$, $y_{y,0} \rightarrow 1$, and the velocity profile becomes increasingly plug-like. As $B \rightarrow 0$, $y_{y,0} \rightarrow 0$, and the velocity approaches that of a Newtonian fluid. The focus of our paper will be on the effects of channel width variations on the basic Poiseuille flow ($B > 0$).

To simplify matters, we will consider the channel to be symmetric about $y = 0$, and the channel wall to be sinusoidally perturbed, i.e. the upper wall is at:

$$y = y_w(x) = 1 - h \cos 2\pi x. \quad (9)$$

The channel is assumed to extend to $x = \pm\infty$, although we shall only consider one period of the wall variation. Assuming periodicity in x and symmetry of the solution about $y = 0$, boundary conditions at the centreline and wall are:

$$\tau_{xy} = 0, \quad v = 0, \quad \text{at } y = 0, \quad (10)$$

$$u = 0, \quad v = 0, \quad \text{at } y = y_w(x) = 1 - h \cos 2\pi x. \quad (11)$$

In the case that $h = 0$, we have a Poiseuille flow with an unyielded plug in the centre of the channel, but for $h > 0$ it is unclear what happens to the plug. We analyse this for the remainder of the paper, starting with $h = O(\delta)$ (in Section 3 below), for which the plug may remain unyielded. In Section 4, we consider larger h , predict eventual breaking of the plug and examine the extensional pseudo-plug solution that is valid when the plug is broken.

3. Small amplitude wall variation: $h = O(\delta)$

It is physically intuitive that, as $h \rightarrow 0$, the unyielded plug of the underlying basic Poiseuille flow should be recovered in any analysis. Further, since a plug region of finite width in the basic flow is indicative of a finite yield stress, we would expect that for a sufficiently small amplitude channel width perturbation, the plug remains intact along the entire length of the channel, i.e. it is physically unreasonable that an infinitesimal perturbation of the channel wall creates the finite stress required to break the plug at every point.

Accordingly, we consider $h \ll 1$, and specifically $h = O(\delta)$. We seek an asymptotic solution with the following structure. First, close to the wall there will exist a yielded region, which to first approximation is a shear flow (outer solution). Second, in the channel centre there will be a rigid plug (also an outer solution), moving at speed u_p , which will be determined. The two outer solutions will be joined at the approximate position of the (naively) perturbed yield surface by an inner solution and matching conditions. We commence with the yielded outer solution.

3.1. Yielded outer solution

We consider regular expansions in δ of form:

$$(p, u, v) = (p_0, u_0, v_0) + \delta(p_1, u_1, v_1) + \delta^2(p_2, u_2, v_2) + \dots$$

and after substituting in (1)–(3) and a little algebra find at $O(1)$:

$$0 = -p_{0,x} + \frac{\partial}{\partial y} \tau_{xy,0}, \quad (12)$$

$$0 = p_{0,y}, \quad (13)$$

$$0 = u_{0,x} + v_{0,y}, \quad (14)$$

$O(\delta)$:

$$0 = -Re[u_0 u_{0,x} + v_0 u_{0,y}] - p_{1,x} + \frac{\partial}{\partial y} \tau_{xy,1} \quad (15)$$

$$0 = p_{1,y} \quad (16)$$

$$0 = u_{1,x} + v_{1,y}, \quad (17)$$

$O(\delta^2)$:

$$0 = -p_{2,x} + \frac{\partial}{\partial y} \tau_{xy,2} + \frac{\partial}{\partial x} \tau_{xx,0}, \quad (18)$$

$$0 = -p_{2,y} + \frac{\partial}{\partial x} \tau_{xy,0} + \frac{\partial}{\partial y} \tau_{yy,0}. \quad (19)$$

$$0 = u_{2,x} + v_{2,y}, \quad (20)$$

The leading order shear stress is given by $\tau_0 = |\tau_{xy,0}|$ and, provided that $\tau_0 > B$, the shear stress components are given

by:

$$\tau_{xy,0} = u_{0,y} + B \operatorname{sgn}(u_{0,y}), \quad \tau_{xy,1} = u_{1,y},$$

$$\tau_{xx,0} = 2 \left(1 + \frac{B}{|u_{0,y}|} \right) u_{0,x},$$

$$\tau_{xy,2} = \left[u_{2,y} + v_{0,x} - B \operatorname{sgn}(u_{0,y}) \frac{2u_{0,x}^2}{u_{0,y}^2} \right].$$

We note that the x -dependency in (12) enters only through the channel width, $y_w(x)$, and thus we can expect that the leading order solution (u_0, v_0) depends on x only through y_w . It follows that

$$u_{0,x} = \frac{\partial u_0}{\partial y_w} y_{w,x} = O(\delta),$$

$$v_0 = \int_1^y v_{0,y} dy = - \int_1^y u_{0,x} dy = O(\delta).$$

Thus, we note that many of the terms in the leading order deviatoric stresses drop one order, i.e. $\tau_{xx,0} \sim O(\delta)$ and many terms drop out of $\tau_{xy,2}$. We also see that the inertial terms in (15) are in fact $O(\delta)$, and belong in the second order problem.

We now assume that $Re \sim O(\delta)$, so that the inertial terms in fact appear only at $O(\delta^3)$, and will play no part.¹ Substituting for the stress components, our sequence of problems simplifies to:

$$0 = -p_{0,x} + u_{0,yy}, \quad (21)$$

$$0 = -p_{1,x} + u_{1,yy}, \quad (22)$$

$$0 = -p_{2,x} + u_{2,yy}, \quad (23)$$

These equations are valid where $|\tau_{xy,0}| > B$, and where $|\tau_{xy,0}| \leq B$, we have simply that $u_{k,y} = 0, k = 0, 1, 2$. In addition, $p_{k,y} = 0, k = 0, 1, 2$, and the velocity field is divergence free at each order. The outer solution is therefore solved straightforwardly, using the boundary conditions $u_k(x, y_w) = 0, k = 0, 1, 2$, and symmetry at $y = 0$.

At leading order, at each $x \in [-1/2, 1/2]$ we have $\tau_{xy,0} = y p_{0,x}$, and:

$$u_0(x, y) = \begin{cases} \frac{B}{2y_y} (y_w - y_y)^2, & y \in [0, y_y], \\ \frac{B}{2y_y} (y_w - y_y)^2 \left[1 - \frac{(y - y_y)^2}{(y_w - y_y)^2} \right], & y \in (y_y, y_w], \end{cases} \quad (24)$$

where y_y is the position of the pseudo-yield surface, where $|\tau_{xy,0}| = B$:

$$y_y = \frac{B}{|p_{0,x}|}, \quad (25)$$

¹ We consider how inertia modifies our solutions, when $Re = O(1)$, later in Section 3.5.

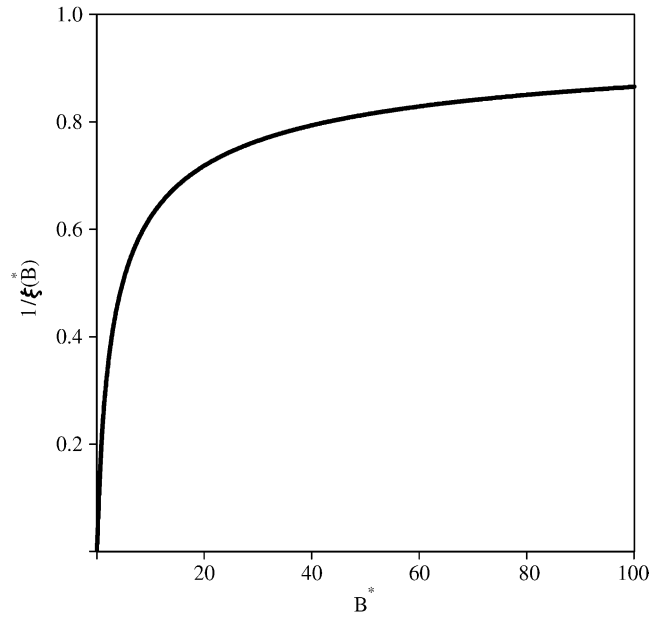


Fig. 2. The function $\xi(B^*)$ that defines $y_y(x)$.

However, $|p_{0,x}|$ is as yet unknown. This is determined from the constraint of a unit areal flux in the x -direction at leading order, (due to scaling with the mean velocity), i.e.

$$\int_0^{y_w} u_0(x, y) dy = 1. \quad (26)$$

After minor manipulations, we find that $y_y = y_w/\xi$, where $\xi = \xi(B^*)$, is the single root of the Buckingham equation:

$$2\xi^3 - \left(3 + \frac{6}{B^*} \right) \xi^2 + 1 = 0, \quad (27)$$

for which $\xi > 1$, and $B^* = B y_w^2$. On finding the root (e.g. numerically, see Fig. 2), we can determine y_y . The pressure gradient is defined by (25), and finally the solution from (24). Thus, the entire leading order solution depends only on B and on $y_w(x)$, as previously stated.

3.1.1. The lubrication paradox illustrated

The zero-th order solution (24), has the characteristic Bingham–Poiseuille velocity profile of a sheared layer with a parabolic variation coupled to a plug region. However, it is evident that the plug region, $y \in [0, y_y]$, is not a true plug region, since the leading order velocity varies in the x -direction. This is the essence of the lubrication paradox for yield stress fluids.

The axial variation in velocity is characterised by that in the channel centre. We denote the pseudo-plug velocity by $u_{pp}(x)$:

$$u_{pp}(x) \equiv u_0(y_y(x)) = \frac{B}{2y_y} (y_w - y_y)^2. \quad (28)$$

Since $y_w = 1 + O(\delta)$, we have that $B^* = B + O(\delta)$ and therefore $\xi(B^*) = 1/y_{y,0} + O(\delta)$, where $y_{y,0}$ is the yield sur-

face in the unperturbed plane channel. It follows that both the pseudo-yield surface position, $y_y(x)$, and pseudo-plug velocity, $u_{pp}(x)$, are $O(\delta)$ perturbations from their unperturbed plane channel values. The lubrication equations were derived under the assumption that the axial velocity is an order of magnitude larger than that across the channel and that all variations in the axial direction are slow in comparison with

those across the channel. The latter assumption breaks down but not the former. Two leading order solutions are illustrated in Fig. 3. We see that the pseudo-plug speed and pseudo-yield surface position essentially follow the channel width variation. The pressure gradient adjusts to force the unit flow rate through the narrower parts of the channel. In turn this results in a narrower pseudo-plug.

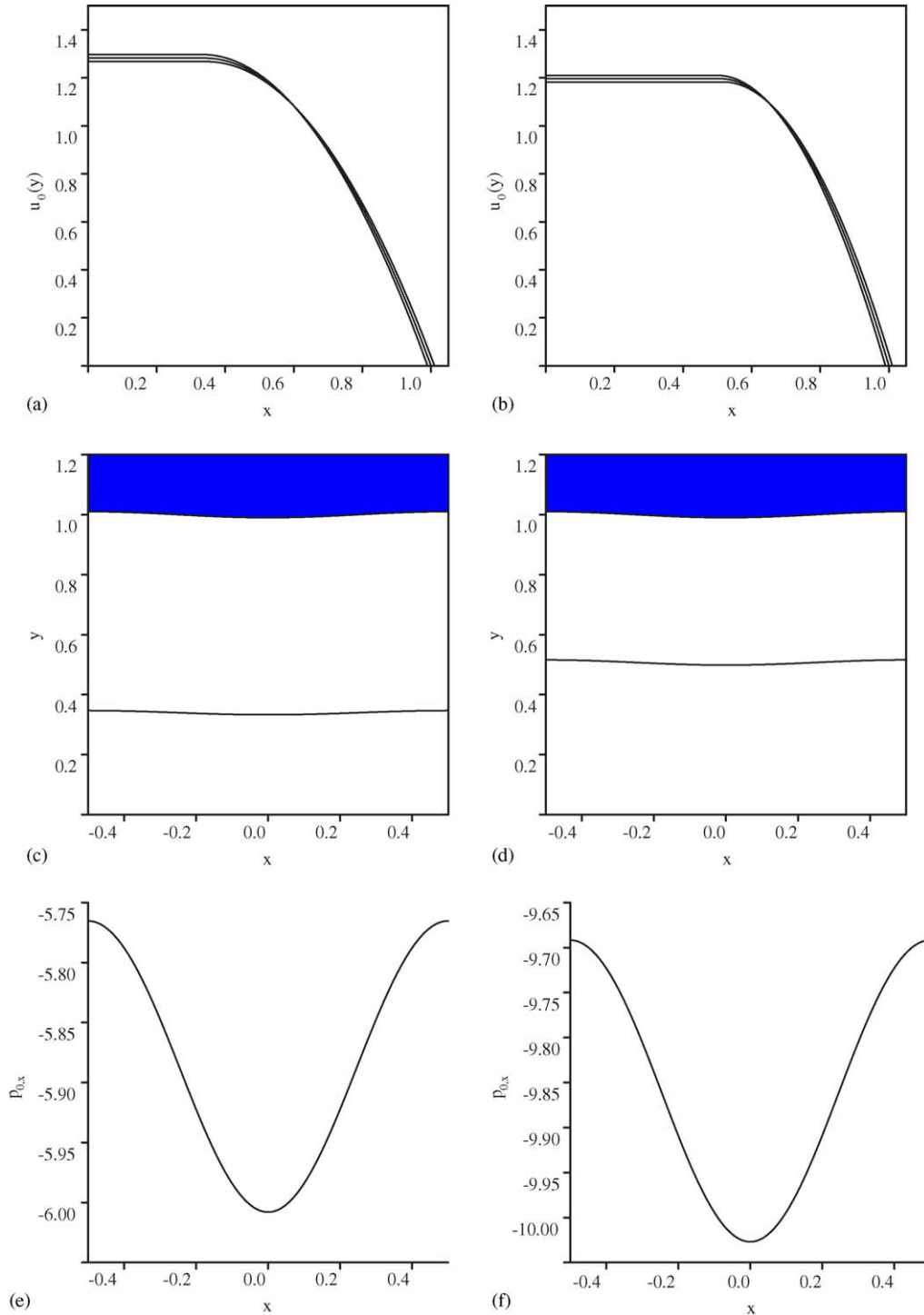


Fig. 3. Leading order outer velocity solution for $\delta = 0.05$, $h = 0.01$, $B = 2$: (a) $u_0(y)$, $y_w(x)$ at $x = 0, 0.25, 0.5$; (c) $y_y(x)$ (shaded area denotes the upper channel wall); (e) $p_{0,x}(x)$; parts (b), (d) and (f) are as (a), (c) and (e) with $B = 5$.

3.2. Higher order corrections: determining the true yield surface

In our leading order solution we have extensional velocity gradients of $O(\delta)$. These balance with gradients in $u_0(y)$, at a distance of $O(\delta)$ from the pseudo-yield surface, $y_y(x)$. This indicates both where the outer expansion breaks down and also the re-scaling needed to resolve the (misnamed) paradox.

Suppose that for sufficiently small $h = O(\delta)$ there is a true plug, intact along the length of the channel, bounded by the yield surface, $y = y_T(x)$. We may assume that $y_T(x)$ lies within $O(\delta)$ of the pseudo-yield surface, $y_y(x)$. Secondly, we can expect that the velocity of the true plug, say u_p , lies somewhere within the range of the pseudo-plug velocities, i.e. there exists $x_p \in [0, 1/2]$:

$$u_p = u_{pp}(x_p) : \quad x_p \in [-1/2, 1/2]. \quad (29)$$

(Note that that since $u_{pp}(x_p) = u_{pp}(-x_p)$, we may take $x_p > 0$ without loss of generality.) With these assumptions, we shall proceed to derive higher order corrections to u_0 and complete our asymptotic solution. However, first consider what the solution and yield surface must look like, in order for a true plug to remain intact along the channel length.

We assume that for the corrected velocity field, the largest velocity at each x will be the plug velocity, u_p , reached at $y_T(x)$. Consider the velocity at a fixed x , for which $u_{pp}(x) > u_p$ (i.e. $|x| < x_p$). The outer solution u_0 is travelling *too fast* in the pseudo-plug. To correct the outer solution, the $O(\delta)$ flux discrepancy $[u_{pp}(x) - u_p]y_y$, must be subtracted from the plug region and added to the flux in the sheared layer, to conserve mass. Thus, the first order velocity correction should be positive in the sheared layer. This suggests that the true plug be wider than the pseudo-plug where $|x| < x_p$. Similarly, for x such that $x_p < |x| \leq 1/2$, so that $u_{pp}(x) < u_p$, we expect the true plug to be narrower than the pseudo-plug. We consider these two cases separately below. We deal later, in Section 3.3, with determination of u_p .

3.2.1. The case $u_{pp}(x) < u_p$, $y_T(x) < y_y(x)$

Here, we assume that:

$$y_y(x) \sim y_T(x) + \delta \xi_T(x) + O(\delta^2), \quad (30)$$

and shall find an expression for $\xi_T(x)$, the first order perturbation from $y_y(x)$. We match our two outer velocity solutions in a transition layer of $O(\delta)$, by assuming a composite solution of form:

$$u \sim \begin{cases} u_p, & 0 \leq y \leq y_T, \\ u_p + \delta^2 u_2^i(x, y) + \dots, & y_T < y \leq y_y, \\ u_0(x, y) + \delta u_1(x, y) \\ \quad + \delta^2 u_2(x, y) + \dots, & y_y < y \leq y_w. \end{cases} \quad (31)$$

We begin by constructing the outer solutions u_1 and u_2 , by defining u_1^* , q_1 , u_2^* and q_2 as follows:

$$u_1(y_y) \equiv u_1^*, \quad \int_{y_y}^{y_w} u_1 \, dy \equiv q_1, \\ u_2(y_y) \equiv u_2^*, \quad \int_{y_y}^{y_w} u_2 \, dy \equiv q_2.$$

Note that for given u_1^* and q_1 , we can solve (22) for u_1 and $p_{1,x}$; similarly (23) for u_2 and $p_{2,x}$. We find that:

$$u_1 = \frac{y - y_w}{(y_w - y_y)^2} \left[u_1^*(3y - 2y_y - y_w) - 6q_1 \frac{y - y_y}{(y_w - y_y)} \right], \quad (32)$$

$$p_{1,x} = -\frac{12q_1}{(y_w - y_y)^3} + \frac{6u_1^*}{(y_w - y_y)^2}, \quad (33)$$

$$u_2 = \frac{y - y_w}{(y_w - y_y)^2} \left[u_2^*(3y - 2y_y - y_w) - 6q_2 \frac{y - y_y}{y_w - y_y} \right], \quad (34)$$

$$p_{2,x} = -\frac{12q_2}{(y_w - y_y)^3} + \frac{6u_2^*}{(y_w - y_y)^2}, \quad (35)$$

The values u_1^* and q_1 are found by matching to the first order inner expansion at y_y , and similarly for u_2^* and q_2 at second order.

In the inner transition layer, we take the expansion

$$u^i = u_p + \delta^2 u_2^i(x, y) + \delta^3 u_3^i(x, y) + \dots, \quad (36)$$

and introduce the inner coordinate ξ :

$$y = y_T(x) + \delta \xi. \quad (37)$$

We substitute the expansion (36) (and equivalent ones for p^i and v^i), into the lubrication equations, expand in powers of δ and collect terms. The y -component of the inner velocity, $v^i \sim O(\delta^3)$, across this layer and hence v^i plays no part. The leading order shear stress is:

$$\tau_{xy} \sim B \text{sign}(u_{2,\xi}^i) + \delta u_{2,\xi}^i + O(\delta^2), \quad (38)$$

and the momentum equations are:

$$0 = -p_{0,x} + u_{2,\xi\xi}^i, \quad (39)$$

$$0 = -p_{0,\xi}. \quad (40)$$

We therefore match $p_{0,x}$ with the outer pressure gradient and integrate out from the true yield surface, $\xi = 0$, at which

$$0 = u_2^i = u_{2,\xi}^i.$$

This gives the following expression for u_2^i :

$$u_2^i = p_{0,x} \frac{\xi^2}{2} = -\frac{B}{2y_y} \xi^2 < 0. \quad (41)$$

At y_y ($\xi = \xi_T$), the velocity and stress for the inner solution are:

$$u^i(y_y) \sim u_p - \delta^2 \frac{B}{2y_y} \xi_T^2 + O(\delta^3), \quad (42)$$

$$\tau_{xy}^i(y_y) \sim -B - \delta \frac{B}{y_y} \xi_T + O(\delta^2). \quad (43)$$

whereas for the outer solution:

$$u(y_y) \sim u_{pp}(x) + \delta u_1^* + \delta^2 u_2^* + O(\delta^3), \quad (44)$$

$$\tau_{xy}(y_y) \sim -B + \delta u_{1,y}(y_y) + \delta^2 u_{2,y}(y_y) + O(\delta^3). \quad (45)$$

Thus, the first order velocity correction compensates for the discrepancy in plug speeds:

$$u_1^* = \frac{1}{\delta} [u_p - u^{pp}(x)], \quad (46)$$

and the $O(\delta^2)$ terms in (42) and (44) yield

$$u_2^* = -\frac{B}{2y_y} \xi_T^2. \quad (47)$$

Hence, $u_1^* > 0$ and $u_2^* < 0$. To find q_1 and q_2 we consider the total areal flux across the channel:

$$\begin{aligned} 1 &= \int_0^{y_w} u \, dy \\ &= \int_0^{y_y} u \, dy + \int_{y_y}^{y_w} u_0 + \delta u_1 + \delta^2 u_2 \, dy + O(\delta^3), \end{aligned} \quad (48)$$

$$= y_y u_p + \int_{y_y}^{y_w} u_0 \, dy + \delta q_1 + \delta^2 q_2 + O(\delta^3), \quad (49)$$

$$= 1 + y_y [u_p - u_{pp}(x)] + \delta q_1 + \delta^2 q_2 + O(\delta^3). \quad (50)$$

Note that we have used the fact that (26) is satisfied for the leading order outer solution (24). Also note that the contribution to the flux from the $O(\delta^2)$ non-constant velocity terms, integrated across the transition layer, is felt at $O(\delta^3)$. Matching the orders above gives:

$$q_1 = -y_y u_1^*, \quad (51)$$

$$q_2 = 0. \quad (52)$$

Finally, ξ_T comes from matching the inner and outer stresses, at first order:

$$-\frac{B}{y_y} \xi_T = u_{1,y}(y_y).$$

The right-hand side can be expressed in terms of u_1^* , and after some algebra, we find:

$$\xi_T = \frac{u_1^*(y_y + 2y_w)}{u_{pp}}, \quad (53)$$

which is $O(1)$ and positive, as required.

3.2.2. The case $u_{pp}(x) > u_p$, $y_T(x) > y_y(x)$

Here, we adopt a similar approach to the previous section. We expect that $y_T(x) > y_y(x)$ and hence write

$$y_T(x) \sim y_y(x) + \delta \xi_T(x) + O(\delta^2), \quad (54)$$

We adopt the following structure for our velocity solution:

$$u \sim \begin{cases} u_p, & 0 \leq y \leq y_T, \\ u_0(y_w(x), y) + \delta u_1(x, y) \\ \quad + \delta^2 u_2(x, y), & y_T < y \leq y_w, \end{cases} \quad (55)$$

and will choose u_1 and u_2 to match the velocity and stress at the yield surface, and the pressure gradients chosen so that the flux constraint is satisfied along the channel. We define u_1^* , q_1 , u_2^* and q_2 as follows:

$$u_1(y_T) \equiv u_1^*, \quad \int_{y_T}^{y_w} u_1 \, dy \equiv q_1,$$

$$u_2(y_T) \equiv u_2^*, \quad \int_{y_T}^{y_w} u_2 \, dy \equiv q_2.$$

As before, in terms of u_1^* , q_1 , u_2^* and q_2 we find:

$$u_1 = \frac{(y - y_w)}{(y_w - y_T)^2} \left[u_1^*(3y - 2y_T - y_w) - 6q_1 \frac{(y - y_T)}{(y_w - y_T)} \right], \quad (56)$$

$$p_{1,x} = -\frac{12q_1}{(y_w - y_T)^3} + \frac{6u_1^*}{(y_w - y_T)^2}, \quad (57)$$

$$u_2 = \frac{(y - y_w)}{(y_w - y_T)^2} \left[u_2^*(3y - 2y_T - y_w) - 6q_2 \frac{(y - y_T)}{(y_w - y_T)} \right], \quad (58)$$

$$p_{2,x} = -\frac{12q_2}{(y_w - y_T)^3} + \frac{6u_2^*}{(y_w - y_T)^2}, \quad (59)$$

In order to have continuity of velocity at y_T we require

$$u_p = u_0(y_T) + \delta u_1^* + \delta^2 u_2^*,$$

which leads to:

$$u_1^* = \frac{1}{\delta} (u_p - u_{pp}(x)), \quad u_2^* = \frac{1}{\delta^2} (u_{pp}(x) - u_0(y_T(x))). \quad (60)$$

Note that both u_1^* and u_2^* are $O(1)$ provided that $y_T - y_y = O(\delta)$, and that $u_1^* < 0$, $u_2^* > 0$. Considering the flow rate through the channel, as in the previous section:

$$\begin{aligned} 1 &= \int_0^{y_w} u \, dy = \int_0^{y_T} u \, dy + \int_{y_T}^{y_w} u \, dy \\ &= y_T u_p + \int_{y_T}^{y_w} u_0 \, dy + \delta q_1 + \delta^2 q_2 + O(\delta^3). \end{aligned} \quad (61)$$

From (26), we have

$$1 = y_y u_{pp} + \int_{y_y}^{y_w} u_0 dy,$$

and hence combining:

$$0 = [u_p - u_{pp}]y_y + \delta q_1 + [u_p - u_{pp}][y_T - y_y] + \delta q_2 + O(\delta^3). \tag{62}$$

Therefore,

$$q_1 = -y_y u_1^*, \quad q_2 = -\xi_T u_1^*. \tag{63}$$

Now ξ_T is found by matching the shear stress to $O(\delta)$ at y_T . This requires that

$$0 = \frac{2\xi_T u_{pp}}{(y_w - y_y)^2} + \frac{2u_1^*(y_y + 2y_w + 2\delta\xi_T)}{(y_w - y_y - \delta\xi_T)^2}. \tag{64}$$

After some algebra, we find:

$$\xi_T = -\frac{u_1^*(y_y + 2y_w)}{u_{pp}}, \tag{65}$$

which is $O(1)$ and positive, as required. The solution is complete provided that the true plug speed may be determined.

3.3. Determination of the true plug speed

Our asymptotic solutions depend only upon the plug speed, u_p , which has not been specified. We have only specified that u_p lies in the range of pseudo-plug speeds, $u_{pp}(x)$. Since for each choice of u_p the solution is fully determined outside the true plug, it appears that to determine u_p we should consider what happens within the plug. However, within the plug deviatoric stresses are indeterminate and hence there is no point considering any pointwise expression. Therefore, we consider the integral form of the x -momentum Eq. (1). We take arbitrary $x_b \in (0, 1/2)$, and evaluate the integral momentum balance over the two plug domains $\Omega_{p,1}(x_b)$ and $\Omega_{p,2}(x_b)$, shown in Fig. 4.

$$\begin{aligned} & \int_0^{y_T(x_b)} J_1(x_b, y) dy \\ &= \int_0^{x_b} [J_2(x, y_T(x)) - J_2(x, 0) + y_T'(x)J_1(x, y_T(x))] dx \\ &+ \int_0^{y_T(0)} J_1(0, y) dy, \end{aligned} \tag{66}$$

$$\begin{aligned} & \int_0^{y_T(x_b)} J_1(x_b, y) dy \\ &= \int_{1/2}^{x_b} [J_2(x, y_T(x)) - J_2(x, 0) + y_T'(x)J_1(x, y_T(x))] dx \\ &+ \int_0^{y_T(1/2)} J_1(1/2, y) dy, \end{aligned} \tag{67}$$

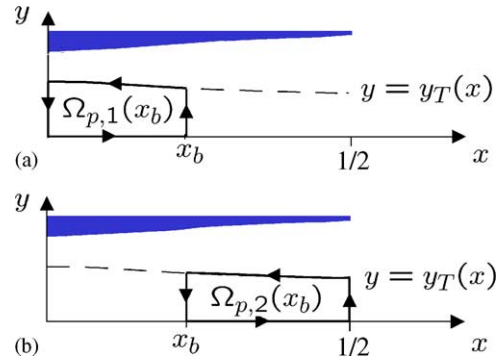


Fig. 4. Contours selected for the evaluation of (66) and (67).

where

$$J_1 \equiv -p + \delta^2 \tau_{xx} - \delta Re u^2, \tag{68}$$

$$J_2 \equiv -\tau_{xy} + \delta Re uv. \tag{69}$$

Within the plug, τ_{xx} is indeterminate, but still single valued. Thus, the expressions on the left-hand side of (66) and (67) must be equal. All other terms in (66) and (67) can be evaluated from the asymptotic solutions of the previous section, or from symmetry considerations. From the symmetry of the flow with respect to $y = 0$:

$$\tau_{xy}(x, 0) = 0, \quad v(x, 0) = 0.$$

Note that since $u(x, y) = u_p$, from the continuity equation $v_y = -u_x = 0$, in the plug and, after integrating, $v = 0$ within the true plug. From the periodicity in x , at the maxima and minima of $y_w(x)$, we have

$$\tau_{xx}(\pm j/2, y) = \frac{\partial \tau_{xy}}{\partial x}(\pm j/2, y) = 0, \quad j = 0, 1, 2, 3, \dots \tag{70}$$

(see also our later discussion of the case $h = O(1)$, in Section 4). The y -momentum equation, at maxima and minima of $y_w(x)$, becomes $p_y = 0$, $j = 0, 1, 2, 3, \dots$. Subtracting (67) from (66), and using the symmetry conditions, we have:

$$\begin{aligned} 0 &= \int_0^{1/2} -\tau_{xy}(x, y_T(x)) \\ &+ y_T'(x)[-p + \delta^2 \tau_{xx} - \delta Re u^2](x, y_T(x)) dx \\ &+ \int_0^{y_T(0)} [-p - \delta Re u^2](0, y) dy \\ &- \int_0^{y_T(1/2)} [-p - \delta Re u^2](1/2, y) dy \end{aligned} \tag{71}$$

Any legitimate choice of u_p must satisfy (71). We integrate by parts the term multiplied by $y_T'(x)$, cancelling out

the integrals at $x = 0, x = 1/2$. This gives:

$$0 = \int_0^{1/2} -\tau_{xy}(x, y_T(x)) + y_T(x) \left[\frac{\partial p}{\partial x}(x) - \delta^2 \frac{\partial}{\partial x} \tau_{xx}(x, y_T(x)) \right] dx, \quad (72)$$

note that u is independent of x along $y = y_T$, and is constant within the true plug. We now substitute our asymptotic solutions in the above integral and retain the leading order terms, which are of $O(\delta)$:

$$0 = \int_0^{1/2} [y_T(x) - y_y(x)] \frac{\partial p_0}{\partial x}(x) + \delta y_T(x) \frac{\partial p_1}{\partial x}(x) dx, \quad (73)$$

Eq. (73) represents a force balance. The net force of the zero-th order pressure gradient, acting on the plug perturbation, and the first order pressure gradient, acting on the full plug, should be zero, i.e. in equilibrium, provided that we have chosen the correct plug speed. The terms on the right-hand side of (73) will depend on the plug speed, or equivalently the position x_p . We therefore define

$$F(x_p) \equiv \int_0^{1/2} [y_T(x) - y_y(x)] \frac{\partial p_0}{\partial x}(x) + \delta y_T(x) \frac{\partial p_1}{\partial x}(x) dx,$$

and seek $x_p \in (0, 1/2)$, for which $F(x_p) = 0$, i.e. Eq. (73). Recall that x_p is defined such that $u_{pp}(x_p) = u_p$, see (29).

Two examples of $F(x_p)$ are shown in Fig. 5. Note that if $x_p = 0$, we will have $u_p > u_{pp}(x)$, $y_T(x) < y_y(x)$, $u_1^* > 0$, $q_1 < 0$ and $p_{1,x} > 0$, at each x (see Section 3.2.1). Consequently, $F(x_p) > 0$ at $x_p = 0$. Conversely, selecting the widest part of the channel, $x_p = \pm 1/2$, we will have $u_p < u_{pp}(x)$, $y_T(x) > y_y(x)$, $u_1^* < 0$, $q_1 > 0$ and $p_{1,x} < 0$, at each x , and therefore $F(x_p) < 0$ at $x_p = 0.5$ (see Section 3.2.2). Thus, there is at least one value of x_p (or u_p), for which $F(x_p)$ vanishes. In fact we may generally expect the variation in $F(x_p)$ to be strictly monotone for $x_p \in (0, 1/2)$, and thus (73) uniquely determines the plug speed. It can be seen in Fig. 5 that the zero of (73) is close to $x_p = 0.25$, which corresponds to the plug speed in the unperturbed uniform

channel. Physically, if we choose u_p too fast or too slow, the net forces in the x -direction are not in equilibrium; there is a single plug speed for which this is achieved.

In Fig. 6, we show the variation of x_p with the parameters B, δ and h . Departures from the plane channel plug speed are observable. Fig. 6a and b indicate that increasing B reduces x_p , which implies an increase in the true plug speed u_p . This effect is larger with larger δ and h , as is to be expected. If B and δ are fixed then h determines the plug speed, u_p . As the ratio h/δ increases we observe a nearly linear decrease in x_p (hence an increase in u_p), see Fig. 6c. This effect is amplified by large B , see Fig. 6d.

3.4. Example solutions

We present two examples of our composite asymptotic solutions, in Fig. 7. We show the corrected velocity compared against the zero-th order approximation $u_0(y, y_w(x))$, at the widest part of the channel, $x = 0$ and $x = 1/2$. The difference in velocity is barely discernible in each case. In contrast, the difference in yield surface position, $y_T(x)$ (Fig. 7c and d, from the pseudo-yield surface), $y_y(x)$, is quite visible. Furthermore, the yield surface variation with x is in the opposite sense to that of the pseudo-yield surface. Although this may appear counter-intuitive, it follows as a consequence of mass conservation and of having an intact plug (see our earlier discussion). In line with this observation, we see that the magnitude of the pressure gradient, $p_x(x) \sim p_{0,x}(x) + \delta p_{1,x}(x)$, is increased in the narrow parts of the channel, see Fig. 6e and f. The pressure gradient perturbation, $\delta p_{1,x}(x)$, acts to accelerate the yielded part of the flow where $|x| < x_p$, and to decelerate the yielded part of the flow where $|x| > x_p$. The size of the perturbation is significant and increases with B .

3.5. Effects of inertia: $Re \sim O(1)$

Although we have ignored inertia, we may readily see that even if $Re \sim O(1)$, inertia does not play a large role for $h = O(\delta)$. Reviewing the procedure in Sections 3.2.1 and 3.2.2, for our asymptotic solutions, we see that inclusion of inertia

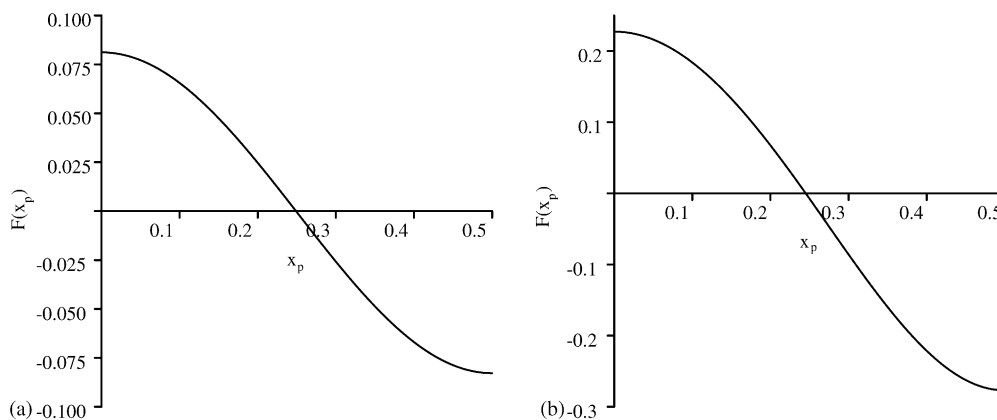


Fig. 5. The function $F(x_p)$ for $\delta = 0.05, h = 0.01$: (a) $B = 2$, ; (b) $B = 5$.

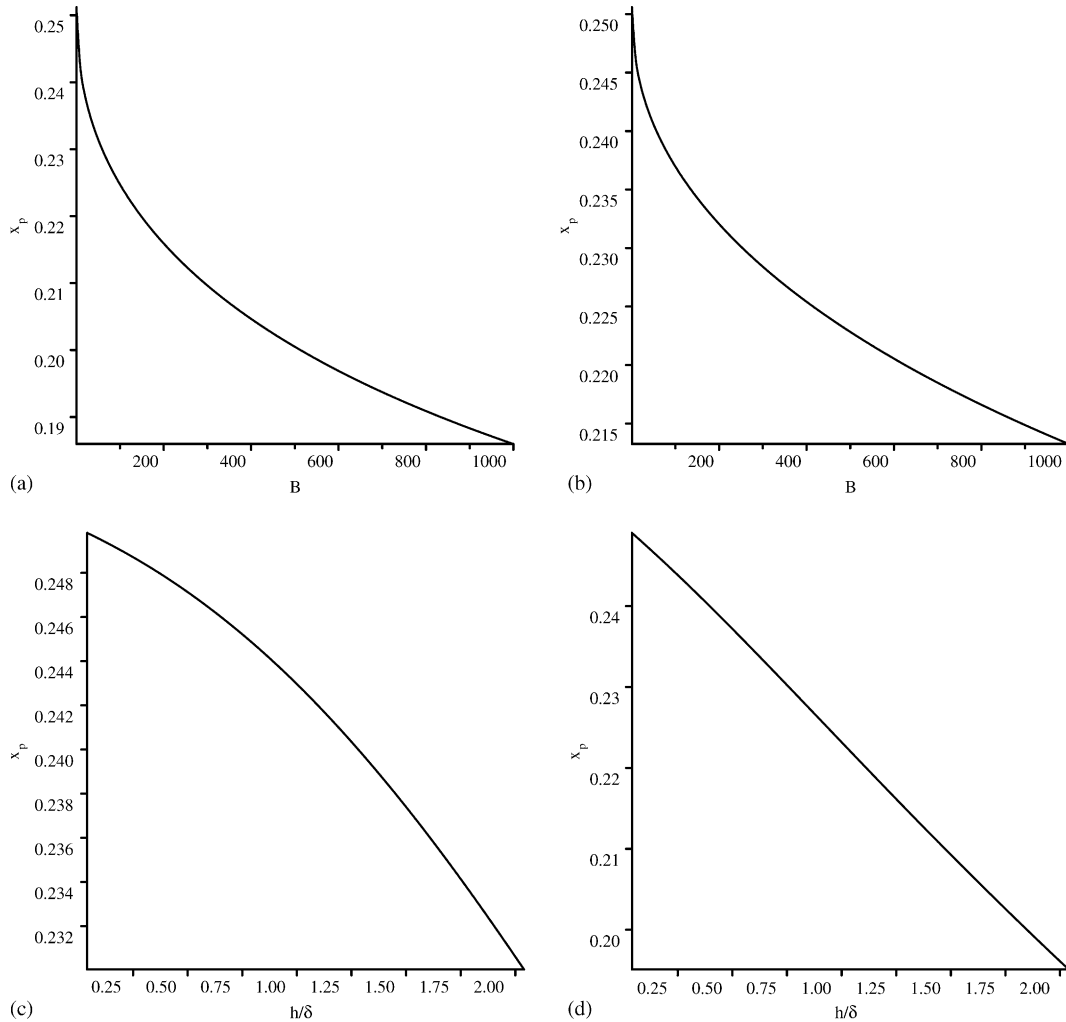


Fig. 6. Variations in x_p with B , δ and h : (a) $\delta = 0.05$, $h = 0.01$, variation with B ; (b) $\delta = 0.02$, $h = 0.005$, variation with B ; (c) $B = 2$, $\delta = 0.05$, variation with h/δ ; (d) $B = 5$, $\delta = 0.05$, variation with h/δ .

will affect only the second order terms. The position of the true yield surface and the selection of the plug speed are determined at first order and hence there is no effect of inertia on these. For $Re \sim O(1)$, the second order velocity profile u_2 and the pressure gradient correction $p_{2,x}$, satisfy:

$$Re \frac{[u_0 u_{0,x} + v_0 u_{0,y}]}{\delta} = -p_{2,x} + u_{2,yy}, \tag{74}$$

with boundary and flux conditions:

Section 3.2.1 : $u_2(y_y) = u_2^*$,

$$u_2(y_w) = 0, \quad \int_{y_y}^{y_w} u_2 dy = q_2, \tag{75}$$

Section 3.2.2 : $u_2(y_T) = u_2^*$,

$$u_2(y_w) = 0, \quad \int_{y_T}^{y_w} u_2 dy = q_2. \tag{76}$$

The values of u_2^* and q_2 are obtained from the same matching conditions as previously in Sections 3.2.1 and 3.2.2. Thus,

we see that inertia acts simply as a localised momentum source in (74). We have not explored these effects further.

4. Breaking the unyielded plug

We have seen in Fig. 7 that although velocity corrections are small, significant modifications to the pressure field are found when the plug remains intact. These pressure gradient perturbations are balanced by shear stress gradients. For sufficiently small h we must assume that the shear stress within the plug remains uniformly below the yield stress. However presumably, as h increases the yield stress will be exceeded within the plug and the plug breaks. Here, we shall assume that there exists a critical amplitude $h = h_c$ at which the true plug is no longer able to remain intact, and we shall estimate h_c .

Suppose that $h < h_c$. If $h \sim O(\delta)$, then our work of the previous section indicates that, as we approach the plug from outside, $\tau_{xy} \sim -B$ and $\tau_{xx} \sim O(\delta)$. Within the true plug, the

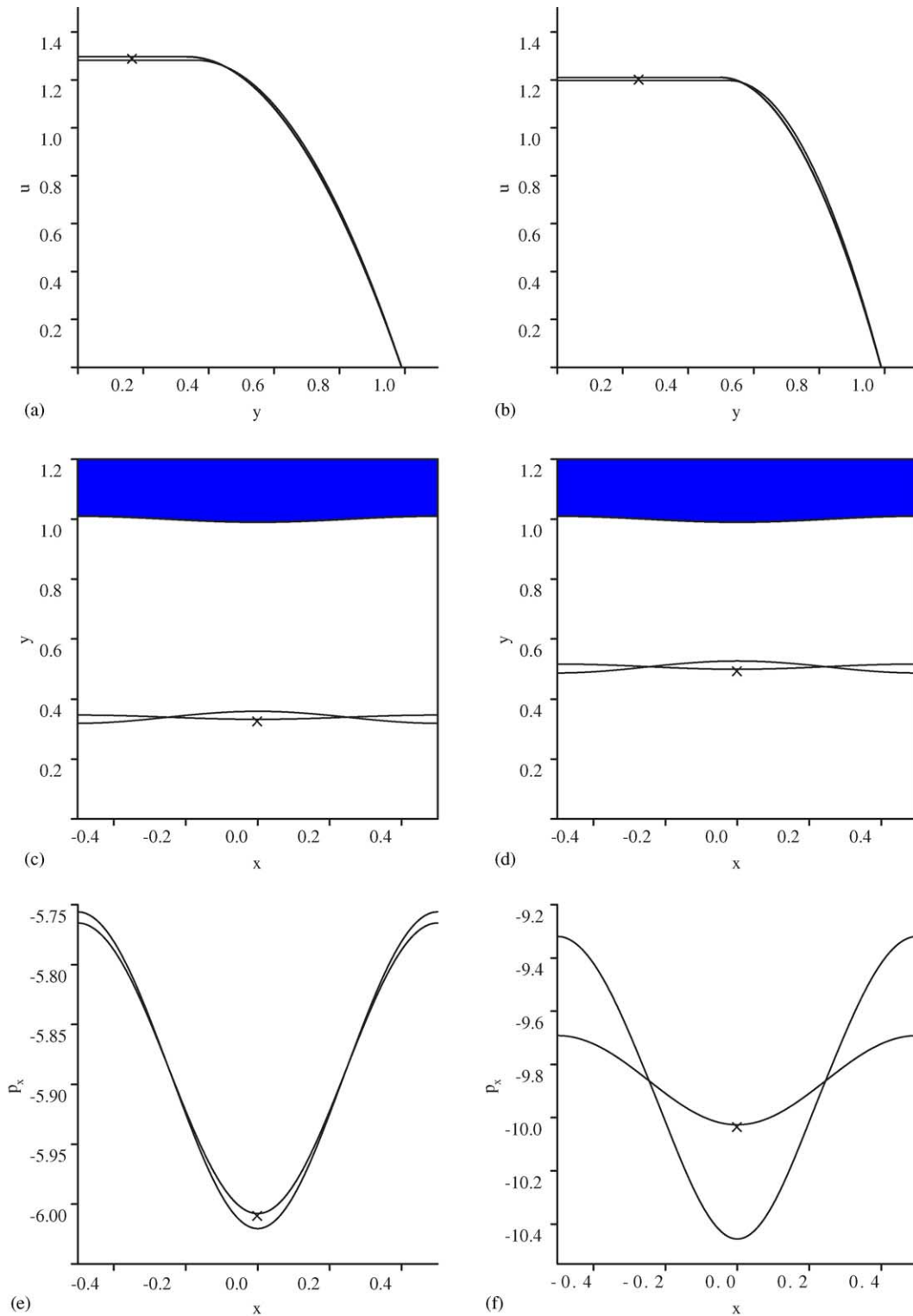


Fig. 7. Composite asymptotic solutions compared with the zero-th order outer approximations (marked with a 'x') for $B = 2$, $\delta = 0.05$, $h = 0.01$: (a) velocity solution at $x = 0$; (c) $y_T(x)$ and $y_b(x)$; (e) pressure gradient. Parts (b), (d) and (f) are as (a), (c) and (e) with $B = 5$.

shear stresses are indeterminate and thus cannot be estimated pointwise. If instead $h > h_c$ the plug breaks somewhere and is replaced by a pseudo-plug region. Within the broken pseudo-plug the flow is extensional and we may deduce that

$\tau_{xx} \sim O(\delta^{-1})$ (see Section 5, following [19]). Therefore, it seems that breaking of the plug occurs when the extensional stresses become $O(\delta^{-1})$ within the plug, but are still $O(\delta)$ outside the plug. To estimate the mean extensional stresses

within the plug we adopt an idea from Szabo and Hassager, on flow in an eccentric annulus [3]. We use the integral momentum balance to estimate the mean extensional stress, τ_{xx} , along a line between $y = 0$ and $y = y_T$, at a fixed point $x = x_b$. When the mean extensional stress exceeds the yield stress, we may conclude that the plug has broken. For given $x_b \in [0, 1/2]$, we define the stress integral $I(x_b)$ by:

$$I(x_b) \equiv \delta \int_0^{y_T(x_b)} \tau_{xx}(x_b, y) dy. \quad (77)$$

A sufficient condition for the plug to have broken (somewhere within the true plug), at point $x = x_b$ is that

$$|I(x_b)| > B y_T(x_b). \quad (78)$$

Note that $|I(x_b)|/y_T(x_b)$ is the mean extensional stress at $x = x_b$. The integral form of the x -momentum equation over $\Omega_{p,1}(x_b)$, as shown in Fig. 4a, gives:

$$\begin{aligned} \delta I(x_b) = & \int_0^{y_T(x_b)} [p + Re\delta u^2] dy \\ & - \int_0^{y_T(0)} [p + Re\delta u^2] dy \\ & - \int_0^{x_b} \tau_{xy}(x, y_T) + y_T' [p(x, y_T) - \delta^2 \tau_{xx}(x, y_T) \\ & + Re\delta u^2(x, y_T)] dx. \end{aligned} \quad (79)$$

We suppose that the left-hand side of (79) will be $O(\delta)$ if h is close to h_c , and accordingly we expand the right-hand side (79) to $O(\delta)$. The term $\delta^2 \tau_{xx}(x, y_T) \sim O(\delta^3)$ and is neglected. We also have that $\tau_{xy}(x, y_T) \sim -B + O(\delta^2) = p_{0,x} y_y(x) + O(\delta^2)$. The inertial terms in the third integral are integrated by parts and cancel with those in the first two integrals. We finally integrate by parts the pressure term. We

find:

$$\begin{aligned} I(x_b) = & \int_0^{x_b} p_{0,x}(x) \frac{[y_T(x) - y_y(x)]}{\delta} \\ & + p_{1,x}(x) y_T(x) dx + O(\delta), \end{aligned} \quad (80)$$

i.e. $I(x_b)$ balances with the net force that results from the action of the zero-th order pressure gradient, acting on the plug perturbation, and the first order pressure gradient acting on the entire plug.

In Fig. 8, we show plots of $I(x_b)$, for two different choices of (B, h, δ) . These plots are qualitatively typical, in that $I(x_b)$ has a single minima and that $I(x_b) = 0$ at $x_b = 0$ and $x_b = 0.5$. In fact, the latter follows automatically from the definition of x_p , (see in Section 3.3). The condition (78), is attained first at the minimum of $I(x_b)$. Differentiating (80), we see that the minimum is when

$$p_{0,x}(x_b) \frac{[y_T(x_b) - y_y(x_b)]}{\delta} + p_{1,x}(x_b) y_T(x_p) = 0, \quad (81)$$

which occurs when $y_T(x_b) = y_y(x_b)$ and $p_{1,x}(x_b) = 0$, i.e. when the zero-th order outer solution coincides with the corrected solution, which occurs only at $x_b = x_p$. This is confirmed numerically. Therefore, we have the interesting result that the position at which the true plug will break is given by $x_b = x_p$. At this point $y_T(x_b) = y_y(x_b)$ and hence the criteria for the plug to break is:

$$\left| \int_0^{x_p} p_{0,x}(x) \frac{[y_T(x) - y_y(x)]}{\delta} + p_{1,x}(x) y_T(x) dx \right| > B y_y(x_b). \quad (82)$$

For fixed (B, δ) , the right-hand side of (82) does not vary with the amplitude h , whereas the left-hand side will increase with amplitude. Therefore, there exists a critical amplitude h_c at which the plug will break. This is found numerically, in a straightforward manner. In Fig. 9, we plot the ratio h_c/δ for $\delta = 0.0001, 0.001, 0.01, 0.05, 0.1$. The ratio h_c/δ decreases

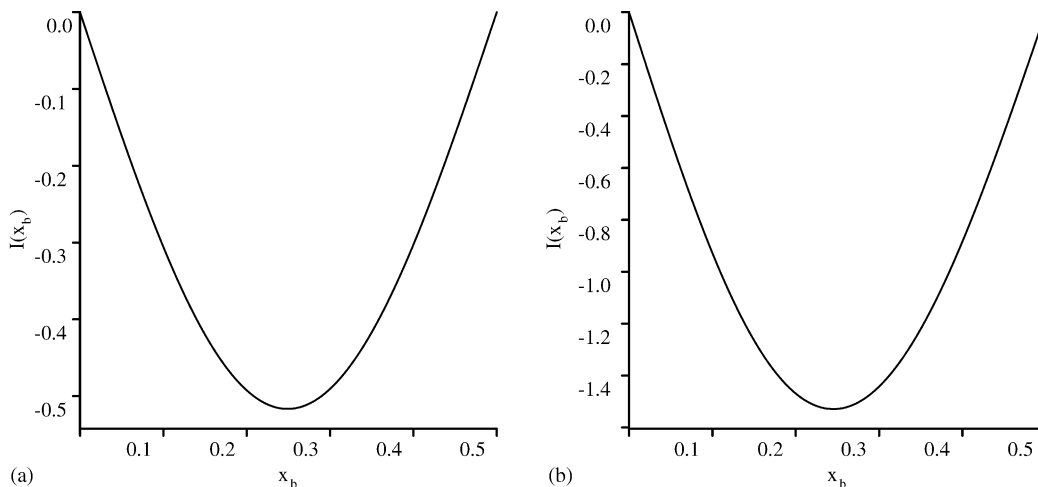


Fig. 8. The function $I(x_b)$: (a) parameters $B = 2, \delta = 0.05, h = 0.01$; (b) parameters $B = 5, \delta = 0.05, h = 0.01$.

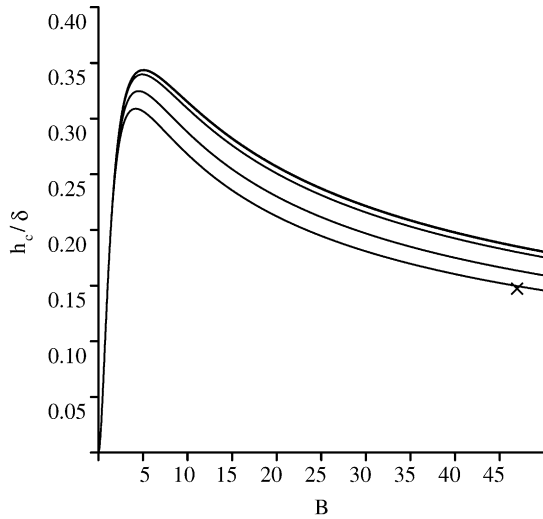


Fig. 9. The critical breaking amplitude h_c , as a function of (B, δ) . Plotted is h_c/δ for $\delta = 0.0001, 0.001, 0.01, 0.05, 0.1$; the curve $\delta = 0.1$ is marked with a 'x'.

slightly with increasing δ . The curves for the two smallest values are indistinguishable and approximately indicate the asymptotic limit. This in itself is interesting. What is also interesting in Fig. 9 is that there is a maximum in the curve $h_c/\delta(B)$, which occurs at $B \approx 5$.

Physically, we might explain the maximum as follows. For small B the plug region is narrower, the yield stress is small and thus the rigid plug is less able to withstand a perturbation of the channel width. As $B \rightarrow 0$ the Newtonian limit is attained, for which there is no plug. As expected, we see that $h_c/\delta(B) \rightarrow 0$. For large B the plug region is large and we expect that the yield stress can withstand a larger perturbation. However, the plug also limits the width of the yielded fluid layer. It is the yielded layer which must compensate for the variations in true plug width and velocity away from the pseudo-plug width and velocity. It does this via the first order perturbation $(u_1, p_{1,x})$. For large B we have seen that the pressure gradient perturbation becomes significant. This contributes to the left-hand side of (82), eventually causing the plug to break. Thus, the yield stress plays a dual role in maintaining/breaking the plug, and the maximal ratio of h_c/δ is found at an intermediate Bingham number.

The limit $h = h_c$ defines an upper bound for the validity of our asymptotic solutions, since these have been derived under the assumption that the plug remains intact. There is however no a priori reason to expect that the solutions break down for $h > h_c$. In Fig. 10, we plot the asymptotic solution for $h = 0.02, 0.05$, for parameters $(B, \delta) = (5, 0.05)$. For these values of (B, δ) , the critical amplitude is $h_c \approx 0.0162$.

Just above the critical amplitude, the solutions still appear physically plausible, see Fig. 10a and b. The perturbation of the velocity appears quite regular. The yield surface and pressure gradient perturbations simply amplify. At larger amplitudes, the correction to the pressure gradient, $\delta p_{1,x}(x)$, becomes of the same order as the zero-th order term, $p_{0,x}(x)$.

Eventually the velocity profiles look unphysical, see Fig. 10c and d, developing discontinuities. These discontinuities are inherent in our perturbation solutions developed in Sections 3.2.1 and 3.2.2. We have stopped at second order and these solutions are C^1 only at first order (since velocity and stress are matched), but higher order terms have not been matched, since we have truncated at second order. Thus, when the higher order terms in the perturbation become large, we see discontinuities in the gradient emerge. These occur at y_y for the solutions in Section 3.2.1 and at y_T for the solutions in Section 3.2.2. For the solutions in Section 3.2.1 this could be improved by a better asymptotic matching procedure (i.e. we have patched the solutions at y_y , rather than matched). However, this seems unnecessary since we have not found unphysical solutions for $h < h_c$.

5. The broken plug: $h = O(1)$

To complete our analysis we consider also the structure of the flow after the plug has broken, $h = O(1) \gg h_c$. For simplicity we consider $Re \ll 1$ and hence the lubrication-scaled Stokes flow problem.² This problem is similar to that analysed in [19], for thin film flow down an inclined plane. Neglecting the inertial terms, (1–2) are replaced by:

$$0 = -\frac{\partial p}{\partial x} + \delta^2 \frac{\partial}{\partial x} \tau_{xx} + \frac{\partial}{\partial y} \tau_{xy}, \quad (83)$$

$$0 = -\frac{\partial p}{\partial y} + \delta^2 \frac{\partial}{\partial x} \tau_{xy} + \delta^2 \frac{\partial}{\partial y} \tau_{yy}. \quad (84)$$

Our focus will be on a cross-section of channel, x , at which there is no true plug region. Following [19], we expect the asymptotic solution to again consist of an outer region close to the wall, where the first approximation is that of a Poiseuille flow in a channel of width $y_w(x)$, another outer region in the channel centre (the pseudo-plug), where the flow is extensional, and an inner region that joins the two outer regions, close to the position of the pseudo-yield surface. The outer solution close to the wall is analogous to that developed in Section 3.1, and the leading order axial velocity is given by (24), which depends only on B and $y_w(x)$. The limiting value of the outer solution as $y \rightarrow y_y(x)$ is again denoted $u_{pp}(x)$, and $u_{pp}(x)$ is largest where the channel is narrowest and vice versa. However now, since $h = O(1)$, the gradient of the axial velocity, $u_{pp,x}(x)$, is no longer $O(\delta)$.

In the pseudo-plug, $0 \leq y < y_y(x)$, we may follow the procedure of [19] and derive the following expressions for the stress and velocity, at leading order:

$$u(x, y) \sim u_{pp}(x) + \delta \left[2|u_{pp,x}|(y_y^2 - y^2)^{1/2} + u_1^* \right] + O(\delta^2), \quad (85)$$

$$v(x, y) \sim -yu_{pp,x}(x) + O(\delta), \quad (86)$$

² We note in passing that, in contrast to when $h = O(\delta)$, inertial effects will be felt at first order, and may be significant. However, this is beyond the scope of our study.

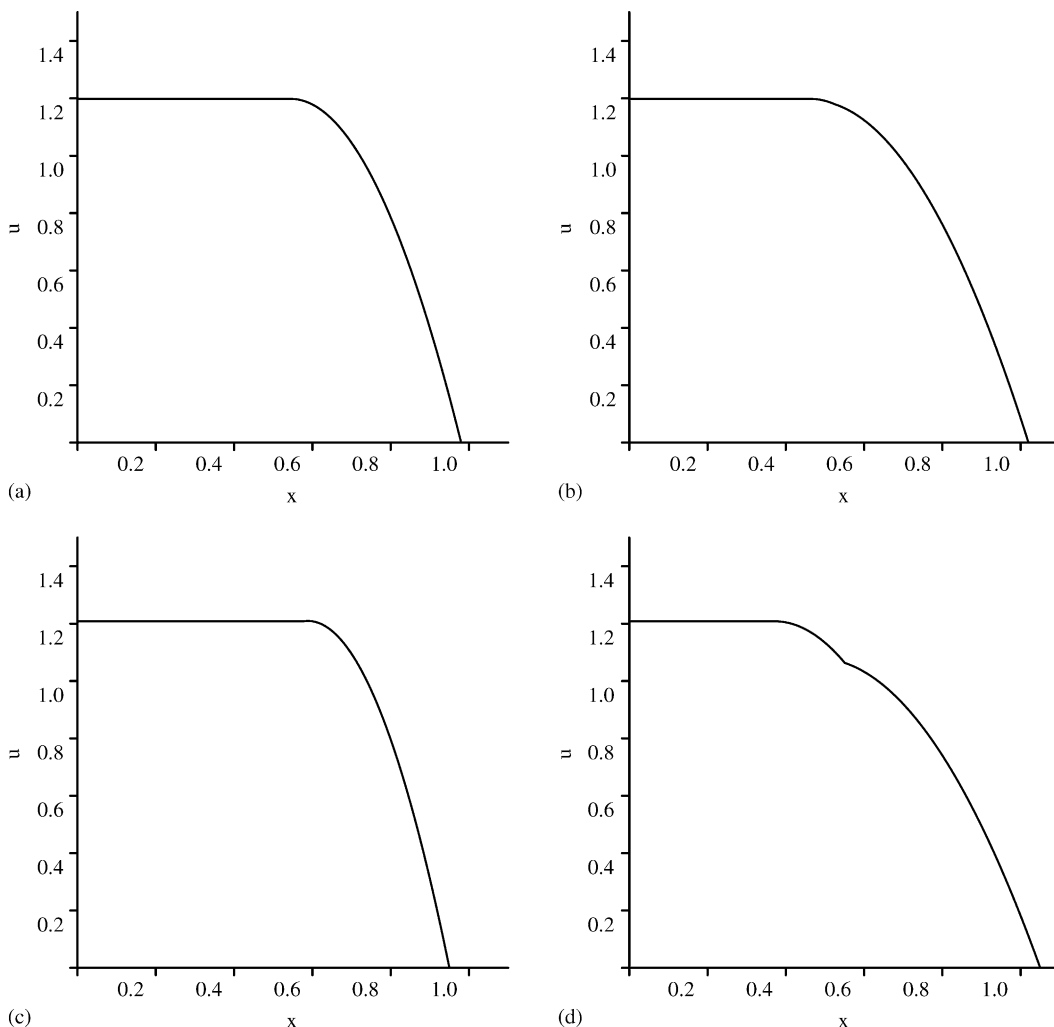


Fig. 10. Velocity solution for $h > h_c \approx 0.0162$ at parameters $B = 5, \delta = 0.05$: (a) $h = 0.02, x = 0$; (b) $h = 0.02, x = 0.5$; (c) $h = 0.05, x = 0$; (d) $h = 0.05, x = 0.5$.

$$\tau_{xy} \sim -\frac{By}{y_y} + O(\delta) \tag{87}$$

$$\tau_{xx} \sim \frac{1}{\delta} \text{sgn}(u_{pp,x}) B \left(1 - \frac{y^2}{y_y^2}\right)^{1/2} + O(1). \tag{88}$$

Thus, we observe that within the pseudo-plug region the leading order stress is exactly equal to the yield stress B . We can develop the series further and will find that

$$\tau \sim B + \delta \frac{\dot{\gamma}_0}{B} + O(\delta^2),$$

where $\dot{\gamma}_0$ is the leading order rate of strain. Thus, the pseudo-plug region is a *slightly yielded* region within which the rates of strain have similar size. However, the flow is still driven by the outer shear flow. For the matching procedure at y_y and further details, we refer to [19].

A key question is whether the above solution describes the flow at each position x , along the channel, i.e. are there any unyielded regions that remain or is the entire channel centre one long extensional flow. The outer shear flow solu-

tion (24) (hence $u_{pp}(x)$ also), depends solely on the channel width $y_w(x)$ and on B . Thus, at the extrema of $y_w(x)$, we have that $u_{pp,x} = 0$. At such points we see that $\tau_{xx} = 0$. Since also $\tau_{xy} = 0$ at $y = 0$, we can assert that there will be unyielded material (a true plug), in some region around the points $(x, y) = (\pm n/2, 0); n = 0, 1, 2, \dots$. Thus, the flow will consist of a mix of yielded shear flow regions, yielded pseudo-plugs and unyielded true plug *islands*, as shown schematically in Fig. 11.

We are unable to specify the exact shape of the true plug regions. Indeed this is one of a number of interesting problems still outstanding for slowly varying/lubrication geometries. However, expanding $y_w(x)$ about a maxima or minima, say $x = x_0$:

$$y_w(x) \sim y_w(x_0) + \frac{(x - x_0)^2}{2} y_{w,xx}(x_0) + O((x - x_0)^3),$$

we see that for $(x - x_0) \sim \delta^{1/2}$, the variation in $y_w(x)$ is $O(\delta h)$. The asymptotic method of Sections 3.2.1 and 3.2.2 is valid for an $O(\delta)$ variation in the channel width. Thus, pre-

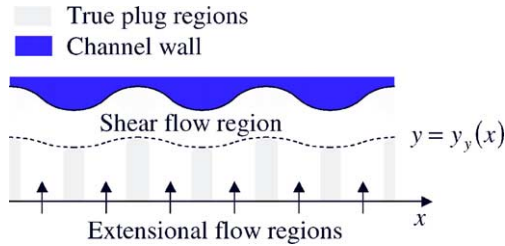


Fig. 11. Schematic of the flow structure for $h = O(1)$, showing the shear flow region, true plug regions at points of symmetry of $y_w(x)$ and extensional flow regions where the analysis in [19] gives the solution.

sumably we could adopt this procedure here, although our procedure for finding the true plug speed needs modifying. This suggests that the true plug islands extend for an $O(\delta^{1/2})$ width about each maxima and minima.

Note that without the asymptotic expressions, we can still infer the structure of the flow from symmetry and continuity arguments. As a Stokes flow we can demonstrate³ uniqueness of the velocity solution and symmetry of the streamlines about $x = 0$ (or indeed any of the extrema of our periodic $y_w(x)$). Thus, we may infer that τ_{xx} changes sign at each extrema of $y_w(x)$. Since also $\tau_{xy} = 0$ along the x -axis, from symmetry and by continuity, we have a sequence of true plug islands surrounding the points $(x, y) = (\pm n/2, 0); n = 0, 1, 2, \dots$, at each of which, $\tau = 0$.

5.1. A necessary condition for the plug to break

From the extensional flow solution (88), we observe that $\tau_{xx} \sim O(\delta^{-1})$ in the extensional pseudo-plug, once the true plug breaks. Integrating $\delta\tau_{xx}$ across the pseudo-plug, at a position x_b , we find that:

$$|I(x_b)| \sim \frac{\pi B y_y(x_b)}{4} + O(\delta), \quad (89)$$

for the broken plug solution. Thus, $|I(x_b)|$ is generally smaller than $B y_y(x_b)$, which is our sufficient condition determining plug-breaking (82). We infer that either: (i) once the plug has broken, the extensional stresses in the pseudo-plug are able to relax to (88), or alternatively, (ii) the condition (82) is sufficient but perhaps not necessary, to break the plug.

³ Uniqueness follows from the formulation of the Stokes flow problem as a minimisation of a convex functional (see e.g. in [27] for more complex visco-plastic problems). The classical arguments for flow symmetry of slow flow of a Newtonian fluid in symmetric geometries (see e.g. [28]), also carry over readily, since these rely partly on uniqueness and partly on being able to reverse the sign of the velocity components. Note that although the equations for the velocity are nonlinear, $\dot{\gamma}$ is unaffected by reversal of flow. We are unaware of these results in the literature, although they seem straightforward and extend to a wide class of generalised Newtonian fluids.

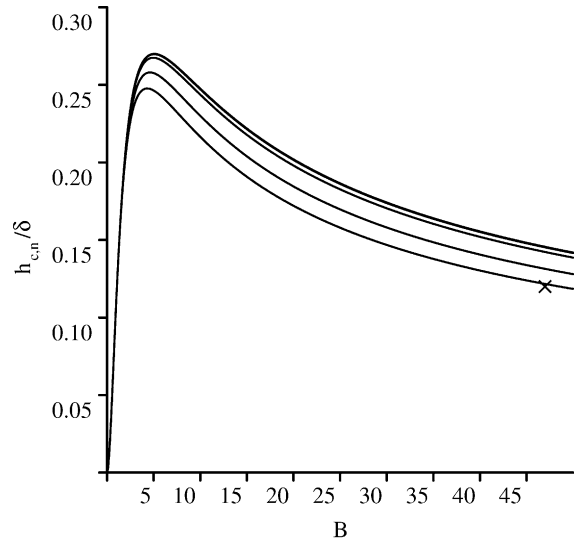


Fig. 12. The necessary condition for the critical breaking amplitude $h_{c,n}$, as a function of (B, δ) . Plotted is $h_{c,n}/\delta$ for $\delta = 0.0001, 0.001, 0.01, 0.05, 0.1$; the curve with $\delta = 0.1$ is marked with a ‘x’.

If we take the second interpretation, a necessary condition to break the plug follows from (89):

$$\left| \int_0^{x_p} p_{0,x}(x) \frac{[y_T(x) - y_y(x)]}{\delta} + p_{1,x}(x) y_T(x) dx \right| > \frac{\pi B y_y(x_p)}{4}. \quad (90)$$

In Fig. 12, we plot the necessary critical amplitude $h_{c,n}$, from criteria (90), for various (B, δ) . The results are similar to Fig. 9, except that evidently $h_{c,n} < h_c$.

6. Discussion

The main contribution of this paper has been to develop an asymptotic solution for the Poiseuille flow of a Bingham fluid down a channel of slowly varying width, in the case that the variation is small. We have shown that an asymptotic solution with an intact true plug region can be found for h less than a critical value $h_c \sim O(\delta)$, and provided upper and lower estimates for h_c . The function h_c/δ shows little variation with $\delta \ll 1$, and exhibits a maximum in B at around $B \approx 5$. In general, there is a small variation in the true plug speed from that of the uniform channel. At small B the perturbed plug moves slightly slower than that in the uniform channel, whereas at large B the true plug moves faster than that in the uniform channel.

After the plug breaks the flow consists of three regions: a shear flow layer close to the wall, unyielded plugs of length $\sim O(\delta^{1/2})$, about each point of symmetry of the periodic wall variation, and extensional flow regions in between. In the extensional flow regions the method of [19] is easily adapted to yield the leading order solution.

Although the picture is largely complete, in so far as small amplitude variations are concerned, there are a number of interesting questions in this area remaining to be studied.

- (1) Generalisation of our analysis to channels with non-symmetrical width variations, i.e. determination of the plug speed and a more general plug breaking criteria.
- (2) Confirmation of our analysis by numerical solution. This is difficult for all the usual reasons that computation of problems with high aspect ratio are difficult. However in addition, an algorithm must be used that computes unyielded regions, e.g. the augmented Lagrangian method.
- (3) Asymptotic analysis of the case, $h \sim h_c$, just after the plug has broken. Since the plug breaks at x_p , the two broken pieces will no longer be constrained to move at speed $u_{pp}(x)$. Presumably there is some form of relaxation. Determination of the new plug speeds and study of transition to the case $h \sim O(1)$ would be of interest.
- (4) Identification of the shape of the true yield surfaces for the case $h \sim O(1)$.
- (5) Consideration of large h , wherein fluid may become stuck on the wall in the wide parts of the channel. This is likely to be associated with flow reversal.

Acknowledgements

This research has been supported financially by Schlumberger and NSERC through CRD project 245434, as well as by the Pacific Institute for the Mathematical Sciences. This support is gratefully acknowledged. S.K. Wilson and B.R. Duffy are thanked for their hospitality and for helpful friendly discussions of the method in [Appendix A](#), and consideration of the extensional flow after breaking of the plug, all during a study visit to the University of Strathclyde in August 2002, (IF). R. Craster is thanked for his lucid explanations of [\[19\]](#). We thank the referees for their helpful comments.

Appendix A. Comparison with the distinguished limit of the bi-viscous model

Lastly we compare the results of [Section 3](#) with the distinguished limit of the bi-viscous model. This asymptotic method was developed in the 1990's in a series of papers by S.D.R. Wilson, [\[7,20,29,30\]](#), and has been used by other authors for a range of lubrication problems, e.g. [\[25,26\]](#). The method is purported to resolve the lubrication paradox, but we shall see that very different results are produced than those in [Section 3](#). In outline, the method is as follows. The lubrication scalings and equations are adopted (identically as we have), but the constitutive laws are replaced by the following bi-viscous model:

$$\tau_{ij} = \left(1 + \frac{B(1-\epsilon)}{\dot{\gamma}}\right) \dot{\gamma}_{ij} \iff \dot{\gamma} > \epsilon B \quad (\text{A.1})$$

$$\tau_{ij} = \frac{\dot{\gamma}_{ij}}{\epsilon} \iff \dot{\gamma} \leq \epsilon B. \quad (\text{A.2})$$

The parameter $\epsilon \ll 1$ represents the ratio between the plastic viscosity in the (dimensional) Bingham model and a bi-viscous *low-shear* viscosity. Thus, the indeterminacy of the exact Bingham model is removed.

The lubrication method proceeds straightforwardly, expanding the momentum equations in powers of the two small parameters, δ and ϵ . It is argued that the correct asymptotic solution will be recovered as the distinguished limit:

$$\epsilon \rightarrow 0, \quad \delta \rightarrow 0, \quad \epsilon = k\delta,$$

where $k \sim O(1)$ is fixed. In application to the channel flow, it is assumed that there is an outer shear layer (in which the treatment is identical to ours earlier), coupled to the pseudo-plug at $y = y_y(x)$. Within the pseudo-plug, we assume

$$u(x, y) \sim u_{pp}(x) + \delta u_1(x, y) + \delta^2 u_2(x, y) + \dots,$$

as before. The leading order approximation to the shear stress, within the pseudo-plug, is found to be:

$$\tau \sim \left[\frac{B^2 y^2}{y_y^2} + 4 \frac{u_{pp,x}^2}{k^2} \right]^{1/2}. \quad (\text{A.3})$$

According to this method, the true yield surface is where $\tau = B$, and thus:

$$y_{T,k} \sim y_y \left[1 - 4 \frac{u_{pp,x}^2}{B^2 k^2} \right]^{1/2}, \quad (\text{A.4})$$

where we have appended the subscript k to distinguish from our earlier expression.

To complete the velocity solution note that for $y \in [0, y_{T,k}(x)]$ the constitutive law is (A.2), whereas in the layer, $y \in (y_{T,k}(x), y_y(x))$, the yield stress is exceeded and the constitutive law is (A.1), as in the outer shear layer. The full expression for the velocity can be evaluated by careful expansion in each region. We find that:

$$u \sim u_0(x, y) + \delta u_1(x, y) + \dots \quad (\text{A.5})$$

$$u_1 = \begin{cases} u_1^* + 2|u_{pp,x}|(y_y^2 - y_{T,k}^2)^{1/2} \\ \quad + \frac{kB}{2y_y}(y_{T,k}^2 - y^2), & y \in [0, y_{T,k}], \\ u_1^* + 2|u_{pp,x}|(y_y^2 - y^2)^{1/2}, & y \in (y_{T,k}, y_y], \\ \frac{(y - y_w)}{(y_w - y_y)^2} \left[u_1^*(3y - 2y_y - y_w) \right. \\ \quad \left. - 6q_1 \frac{(y - y_y)}{(y_w - y_y)} \right], & y \in (y_y, y_w], \end{cases} \quad (\text{A.6})$$

where $u_0 = u_0(y, y_w(x))$ is again given by (24). The parameters u_1^* and q_1 are determined according to continuity and to conserve the unit flow rate; they have the identical meaning as previously, but different expressions.

A number of comments are due. First of all, the expression for the yield surface (A.4) is completely different to ours, in that $y_{T,k}(x) < y_y(x)$ always. If we consider $h = O(\delta)$ then the leading order perturbation of the yield surface disappears and we have $y_{T,k}(x) \sim y_y(x)$, for finite $k > 0$, i.e. the distinguished limit method does not predict any perturbation of the true yield surface from the pseudo-yield surface, let alone a variation in the true yield surface that is in the opposite sense to that in $y_y(x)$.

It might be argued that (A.4) is better suited to the case $h = O(1)$. Indeed, in such fully yielded extensional regions the first order velocity perturbation will coincide with (85). It can be seen that for $h = O(1)$, we have $u_{pp,x} \sim O(1)$ and so the true yield surface may vanish for some interval of x about the point where $|u_{pp,x}|$ is maximal. However, there appears to be no reason to expect that (A.4) has any physical meaning⁴ for the exact Bingham model.

If we believe that $y_{T,k}$ has meaning as a yield surface of some description, we must ask how k is to be selected, independently of δ . This then is the chief problem with the distinguished limit approach. It is sometimes argued that the limit $k \rightarrow 0$, should correspond to the exact Bingham model. Here, we see that this argument is erroneous. Taking $k \rightarrow 0$ in (A.4) will produce $y_{T,k} = 0$ everywhere, except where $y_{w,x} = 0$. As $k \rightarrow 0$ the yield surfaces will be found to surround plug regions that are progressively narrow, located about each point of symmetry of the wall variation. However, we have seen that for the exact Bingham model, purely from symmetry arguments, that a true plug region will remain about each point of symmetry, extending out to $y_y(x)$. From our asymptotic solution, we have argued that these regions should have width $\sim O(\delta^{1/2})$ when $h \sim O(1)$. Thus, selection of k cannot be independent of δ if it is to correctly represent the true plug region.

References

- [1] G.G. Lipscomb, M.M. Denn, Flow of Bingham fluids in complex geometries, *J. Non-Newtonian Fluid Mech.* 14 (1984) 337–346.
- [2] I.C. Walton, S.H. Bittleston, The axial flow of a Bingham plastic in a narrow eccentric annulus, *J. Fluid Mech.* 222 (1991) 39–60.
- [3] P. Szabo, O. Hassager, Flow of viscoplastic fluids in eccentric annular geometries, *J. Non-Newtonian Fluid Mech.* 45 (1992) 149–169.
- [4] G.H. Covey, B.R. Stanmore, Use of the parallel-plate plastometer for the characterisation of viscous fluids with a yield stress, *J. Non-Newtonian Fluid Mech.* 8 (1981) 249–260.
- [5] E.J. O'Donovan, R.I. Tanner, Numerical study of the Bingham squeeze film problem, *J. Non-Newtonian Fluid Mech.* 15 (1984) 75–83.
- [6] D.K. Gartling, N. Phan-Thien, A numerical simulation of a plastic fluid in a parallel-plate plastometer, *J. Non-Newtonian Fluid Mech.* 14 (1984) 347–360.
- [7] S.D.R. Wilson, Squeezing flow of a Bingham material, *J. Non-Newtonian Fluid Mech.* 47 (1993) 211–219.
- [8] J.D. Sherwood, D. Durban, Squeeze flow of a power-law viscoplastic solid, *J. Non-Newtonian Fluid Mech.* 62 (1996) 35–54.
- [9] J.D. Sherwood, D. Durban, Squeeze-flow of a Herschel–Bulkley fluid, *J. Non-Newtonian Fluid Mech.* 77 (1998) 115–121.
- [10] D.N. Smyrniotis, J. Tsamopoulos, Squeeze-flow of Bingham plastics, *J. Non-Newtonian Fluid Mech.* 100 (2001) 165–190.
- [11] K.F. Liu, C.C. Mei, Slow Spreading of a Sheet of Bingham fluid on an inclined plane, *J. Fluid Mech.* 207 (1989) 505–529.
- [12] K.F. Liu, C.C. Mei, Approximate equations for the slow spreading of a thin sheet of Bingham plastic fluid, *Phys. Fluids A2* (1990) 30–36.
- [13] P. Coussot, S. Proust, Slow, unconfined spreading of a mud flow, *J. Geophys. Res.* 101 (1996) 25217–25229.
- [14] P. Coussot, S. Proust, C. Ancey, Rheological interpretation of deposits of yield stress fluids, *J. Non-Newtonian Fluid Mech.* 66 (1996) 55–70.
- [15] J.M. Piau, Flow of a yield stress fluid in a long domain. Application to flow on an inclined plane, *J. Rheology* 40 (1996) 711–723.
- [16] R.W. Griffiths, J.H. Fink, Solidifying Bingham extrusions: a model for the growth of silicic lava domes, *J. Fluid Mech.* 347 (1997) 13–36.
- [17] X. Huang, M.H. Garcia, A Herschel–Bulkley model for mud flow down a slope, *J. Fluid Mech.* 374 (1998) 305–333.
- [18] S.D.R. Wilson, S.L. Burgess, The steady, spreading flow of a rivulet of mud, *J. Non-Newtonian Fluid Mech.* 79 (1998) 77–85.
- [19] N.J. Balmforth, R.V. Craster, A consistent thin-layer theory for Bingham plastics, *J. Non-Newtonian Fluid Mech.* 84 (1999) 65–81.
- [20] S.D.R. Wilson, A note on thin-layer theory for Bingham plastics, *J. Non-Newtonian Fluid Mech.* 85 (1999) 29–33.
- [21] R.W. Griffiths, The dynamics of lava flows, *Annu. Rev. Fluid Mech.* 32 (2000) 477–518.
- [22] N.J. Balmforth, A.S. Burbidge, R.V. Craster, J. Salzig, A. Shen, Viscoplastic models of isothermal lava domes, *J. Fluid Mech.* 403 (2000) 37–65.
- [23] N.J. Balmforth, R.V. Craster, Dynamics of cooling domes of viscoplastic fluid, *J. Fluid Mech.* 422 (2000) 225–248.
- [24] C.C. Mei, M. Yuhi, Slow flow of a Bingham fluid in a shallow channel of finite width, *J. Fluid Mech.* 431 (2001) 135–159.
- [25] A.B. Ross, S.K. Wilson, B.R. Duffy, Thin-film flow of a viscoplastic material round a large horizontal stationary or rotating cylinder, *J. Fluid Mech.* 430 (2001) 309–333.
- [26] S.K. Wilson, B.R. Duffy, A.B. Ross, On the gravity-driven draining of a rivulet of viscoplastic material down a slowly varying substrate, *Phys. Fluids* 14 (2002) 555–571.
- [27] G. Duvaut, J.L. Lions, *Inequalities in Mechanics and Physics*, vol. 219, Springer-Verlag, 1976, pp. 279–327.
- [28] E. Guyon, J.-P. Hulin, L. Petit, C. Matescu, *Physical Hydrodynamics*, Oxford University Press, 2001.
- [29] S.D.R. Wilson, A.J. Taylor, The channel entry problem for a yield stress fluid, *J. Non-Newtonian Fluid Mech.* 65 (1999) 165–176.
- [30] M.A.M. Al Khatib, S.D.R. Wilson, The development of Poiseuille flow of a yield stress fluid, *J. Non-Newtonian Fluid Mech.* 100 (2001) 1–8.

⁴ Obviously there is physical meaning in this expression if we consider a fluid with rheology that is approximated by the appropriate bi-viscous model.